

## The High-Temperature Phases of Sodium Niobate and the Nature of Transitions in Pseudosymmetric Structures\*†

BY I. LEFKOWITZ‡, K. ŁUKASZEWICZ§ AND HELEN D. MEGAW

*Crystallographic Laboratory, Cavendish Laboratory, Cambridge, England*

(Received 20 July 1965)

The lattice parameters of  $\text{NaNbO}_3$  (which has a perovskite structure and is antiferroelectric at room temperature) have been measured by single-crystal X-ray methods from room temperature to  $800^\circ\text{C}$ . While the measurements are in substantial agreement with earlier work, the greater resolution shows up new details, and the interpretation of the earlier work has to be very seriously revised, particularly as concerns the symmetry of the high-temperature phases.

Below the  $360^\circ\text{C}$  transition a second very similar phase  $Q$  can sometimes replace the normal room-temperature phase  $P$ .  $Q$  is believed to be the 'forced ferroelectric' known to be produced from  $P$  by the action of an electric field; the field-free  $P-Q$  transitions are influenced by temperature but have not a reproducible transition temperature.

Above  $360^\circ\text{C}$  there are a large number of transitions characterized by very different features. The facts from this and earlier work are critically reviewed. While the effects cannot yet be explained in detail, the general reasons for expecting such behaviour are discussed. No detailed structural work is reported, but there is evidence for the persistence of Nb displacements above  $360^\circ\text{C}$ , which is therefore not the paraelectric transition.

The transitions in a pseudosymmetric structure cannot be explained or predicted in terms of conventional or macroscopic theories which disregard structural details. A new empirical approach is needed, for which this system provides useful material.

### 1. Introduction

#### 1.1. General aim

Sodium niobate,  $\text{NaNbO}_3$ , is a polymorphous substance which has attracted considerable interest for its electrical properties. All its different structures belong to the perovskite family and are related by displacive or pseudosymmetric transitions. The energy differences must be small, yet they may be associated with very distinct changes of particular properties. It is important therefore to consider what we mean by a phase transition.

Ideally, a displacive phase transition may be defined as a process involving a discontinuous change in at least one atomic position parameter under constant or smoothly changing conditions, any such parameter change being small enough to leave the essential topology of the structure unaltered. Practically, changes in atomic parameters are among the hardest properties to measure; therefore as evidence of a transition we may accept discontinuities in any properties likely to be influenced by discontinuities in atomic parameters. Perhaps the most important of such properties are the

lattice parameters, and they are the main subject of this study. It does not always follow that they are the most sensitive indicators of a transition. Not only may some techniques for studying them have insufficient resolution (which explains some of the discrepancies in the early literature), but it can also happen that lattice parameters are insensitive to certain changes in atomic parameters which alter other properties, for example the refractive index, very appreciably. It is therefore important to compare the results of studies of as many different properties as possible before drawing conclusions.

From a macroscopic standpoint, the classification of a transition as first-order or second-order depended originally on whether there were discontinuities in the free energy or merely in its temperature derivatives; but since direct experimental evidence is hard to obtain, and methods for it are generally insensitive, the definition is usually extended to admit evidence of discontinuities in other macroscopic properties – such as the lattice parameters – which may determine or be determined by the free energy. Obviously when changes are close to the limits of experimental resolution for some properties, the evidence may be contradictory. A transition may be second-order to the degree of approximation in one study, first-order in another. Moreover, the conditions assumed in any theoretical treatment using the distinction may then be unrealizable in practice. Small transitions are certainly influenced by small variations in conditions – for example, by local mechanical stresses or local temperature inhomogeneities –

\* A report giving fuller details of experimental methods and observations may be obtained on application to the Secretary of the Crystallographic Laboratory.

† Research supported in part by the U.S. Department of the Army through its European Research Office.

‡ Present address: Pitman-Dunn Laboratory, Frankford Arsenal, Philadelphia, Pa., U.S.A.

§ On leave of absence from the Institute of Structural Research, Polish Academy of Sciences, Wrocław.

and these may act to 'smear out' discontinuities. The experimental difficulty in deciding about the reality of small discontinuities is in fact related to the theoretical difficulty of enumerating all the variables likely to be relevant. In the present state of knowledge it is more important to get a good experimental description of the features of a transition than to try to decide its order.

The aims of the present study were therefore to find the lattice parameters of  $\text{NaNbO}_3$  with high accuracy from room temperature to about  $800^\circ\text{C}$ ; to find the temperatures at which discontinuities occurred, and the nature of the changes involved; and to pick out the characteristic features by which the different phases could be identified. Earlier studies by others (see § 1.2) had relied on powder diffraction. Our original intention was to use diffraction by single crystals, but it became apparent when we started that it was generally more useful, as well as more practicable, to study lightly twinned crystals by the diffraction techniques appropriate for single crystals. Obviously it would be desirable to determine also the structures of the high-temperature phases, and the changes of atomic parameters at the transitions, but this has to be left to future study, though a little incomplete information about it is reported below. On the other hand, our results for lattice parameters, used in comparison with the earlier work of others, allow some apparent discrepancies to be resolved and a more complete and comprehensive survey of the system as a whole to be given.

### 1.2. Summary of earlier work\*

A survey by Jona & Shirane (1962) reports the relevant experimental work up to 1960, but is not a safe starting-point because its summary of the facts is affected by the implicit underlying assumption of an oversimplified crystal structure. Dielectric measurements by Matthias (1949) and Matthias & Remeika (1951) having aroused interest in the material, pioneer work on its X-ray powder pattern and optical birefringence was done by Wood (1951). Important later studies were made by Shirane, Newnham & Pepinsky (1954) (X-ray powder diffraction, birefringence, and dielectric constant); Cross & Nicholson (1954, 1955) (birefringence, dielectric constant); Francombe (1956) (X-ray powder diffraction); Reisman, Holtzberg & Banks (1958) (differential thermal analysis); Solov'ev, Venevcev & Ždanov (1961) (X-ray powder diffraction); Ismailzade (1963) (X-ray powder diffraction). Studies by Jona, Shirane & Pepinsky (1955) and Wood, Miller & Remeika (1962), mainly concerned with room-temperature effects, are also relevant.

The results of these studies will be described below, in comparison with our results. All reported measurements are in reasonable agreement with ours, when allowance is made for the different sensitivities and resolution of the various methods, except for the work

of SVŽ between  $360^\circ\text{C}$  and  $440^\circ\text{C}$ , and that of Ismailzade (1963) over most of the range, for which see § 5.4.

The conclusions drawn from their measurements by the various authors need to be re-examined, however. Many of them were admittedly provisional, but many were implicitly based on assumptions of simplicity in the system, or on analogies with other simpler systems, which cannot now be taken for granted.\*

### 1.3 Nature of variations in the perovskite family

For any structure family, we call the simplest and most symmetrical structure which retains the essential topology of the family the *aristotype* (implying that the most symmetrical structure is the *best* – Greek, *αριστος*). All variants are called *hettotypes* (*ήττος*, less good).

The aristotype of the perovskite family is otherwise known as the 'ideal perovskite structure'. It is cubic, with a unit-cell side of about  $4 \text{ \AA}$ , and cell contents  $\text{ABO}_3$ ; all atoms are in special positions. The small atom B lies at the centre of an octahedron with oxygen at the corners, each linking two octahedra; the large atom A is in the interstice between octahedra; and all octahedra are identical in shape and orientation.

Hettotypes of the perovskite family may be of various kinds. In some of the simplest, the  $4 \text{ \AA}$  cube is distorted in different ways, but remains the true repeat unit; such structures are *unipartite* in all directions. In others, a sequence of two or more of the original units is needed to form the true repeat unit, and this may be so independently in more than one axial direction; the original unit is now a subcell of the true unit cell, which is *bipartite* or *multipartite* in the direction concerned. Two hettotypes are only different if they have different geometry or symmetry, *i.e.* if they need a geometrically different set of arbitrary parameters to describe them and do not merely differ in the values of the parameters.

Structurally, the features distinguishing hettotypes of  $\text{NaNbO}_3$  from the aristotype may be of different kinds:

- (i) Homogeneous distortion of the whole structure.
- (ii) Displacement of Nb atoms relative to their octahedron centres.
- (iii) Tilting of octahedra relative to one another.
- (iv) Distortions of octahedra not due to (i).
- (v) Displacement of Na atoms and consequent alteration of their environments.

\* *Note added in proof:* – Since this paper was submitted our attention has been called to a recent publication by Tennery (1965) involving study of lines  $N=12$  and  $N=16$  by powder diffractometry. His experimental results are in complete agreement with ours, so far as the different limitations of the two experimental techniques allow. They confirm the discontinuity of the transition near  $360^\circ\text{C}$ , and emphasize its thermal hysteresis; and they indicate the existence of other transitions at  $420$ ,  $527$  and  $576^\circ\text{C}$ , as well as  $640^\circ\text{C}$  (*cf.* § 6.2), adding more detailed information about the temperature ranges and sharpness. His deductions about the symmetry above  $360^\circ\text{C}$  do not follow from the evidence; no such deductions can be legitimately made, for reasons mentioned in §§ 1.2 and 6.1.

\* Papers listed here will be referred to later by initials and dates only, if there is more than one author.

These features may occur singly or in combination. The older ideas considered only (i) and (ii), allotting only one component to the latter. This limitation restricts the number and the nature of the hettotypes which can be envisaged, and has led to various misconceptions: such, for example, as the assumption that there is always (and not merely in a few special cases) a one-to-one correspondence between homogeneous distortion and Nb displacement; or the incorrect statement that a structure with 'superlattice lines' (*i.e.* difference reflexions, indicating a multipartite unit cell) could not be ferroelectric. In fact the enumeration of the possible hettotypes with multiplicity no higher than  $2 \times 2 \times 2$  would be quite tedious – they would include ferroelectric, antiferroelectric and paraelectric – and there are no physical reasons forbidding higher multiplicities. We have still far too few examples to be sure which macroscopic properties are associated with which structural features: to tell, for instance, whether lattice expansions or shears are due to the Nb displacements or to tilting of the octahedra; and whether the tilting is to be treated as an independent variable or is itself a function of the preferred bond-angle at the O atom and/or at the Na–O environment. While examples are accumulating, we have to be particularly careful to record the observed facts as such, and not to translate them prematurely into terms of some oversimplified assumption.

#### 1.4. Axes of reference

It is convenient to keep corresponding axes of reference for the whole series of phases, defined in direction by the edges of the subcell approximating to a  $4 \text{ \AA}$  cube. These are the *pseudocubic* axes\* (unless the unit cell or subcell is a cube, when they become the cubic axes). The subcell edges,  $x$ ,  $y$ ,  $z$ , are taken as units of length in the three axial directions. The true cell edges  $a$ ,  $b$ ,  $c$ , in the same directions are given by

$$a = m_1 x, \quad b = m_2 y, \quad c = m_3 z,$$

where the multiplicities  $m_1$ ,  $m_2$ ,  $m_3$ , are small integers (possibly unity).

We construct the reciprocal lattice corresponding to the subcell. All main reflexions have integral indices  $hkl$ , which are the same throughout the system (except for possible permutations), but there are also difference reflexions with fractional indices having denominators  $m_1$ ,  $m_2$ ,  $m_3$ . These non-integral indices of course do not imply disorder or any kind of anomaly; they are a consequence of our chosen unconventional (but convenient) notation.

\* Such axes have sometimes been called "monoclinic" or 'pseudomonoclinic' axes, but the former name only applies narrowly to one particular group of hettotypes, and the latter is in any case misleading, and both should now be dropped; the term pseudocubic is sufficiently general to use for all symmetries except cubic.

#### 1.5. Room-temperature phases

The normal room-temperature structure was first studied by Vousden (1951); it was examined in more detail by Wells & Megaw (1961) and a redetermination and refinement was made by Łukaszewicz, Sakowski & Megaw (paper in preparation). It is orthorhombic, with symmetry directions  $[10\bar{1}]$ ,  $[010]$ ,  $[101]$ , multiplicities  $m_1=2$ ,  $m_2=4$ ,  $m_3=2$ , and a  $B$ -face-centred lattice. The relation in the (010) plane of the pseudocubic axes and the conventional orthorhombic axes is shown in Fig. 1. The space group is No. 57; with the conventional orthorhombic axes shown, its symbol is  $Pbma$ .

Atomic displacements are such that the octahedra remain nearly regular, but are tilted relative to one another about  $[010]$  and  $[10\bar{1}]$ . Nb atoms have a large displacement component parallel to  $[10\bar{1}]$  and a smaller one parallel to  $[101]$ . Adjacent octahedra are related by a (010) mirror plane; pairs so formed are related by the  $[010]$  screw diad, giving Nb displacements which are antiparallel to those of the first pair. The quadripartite  $b$  edge is both a physically important and an easily detectable feature.

The structure of  $(K_{0.025}Na_{0.975})NbO_3$  was also found by Wells & Megaw (1961) (detailed paper in preparation). This, called phase II, is closely related to the normal structure, but its unit cell is bipartite where the normal structure is quadripartite, *i.e.*  $m_2=2$ ; and it has lower symmetry, belonging to space group no. 26 (with symbol  $P2_1ma$  when conventional orthorhombic axes are used). The large  $[10\bar{1}]$  components of the Nb displacement are now all parallel, with the result that the crystal is ferroelectric.

It was shown by Cross & Nicholson (1954, 1955) that the application of a strong field converts  $NaNbO_3$  at room temperature to a new phase, the 'forced ferroelectric'. This has almost certainly the same structure as phase II (for history and confirmatory evidence, see Wood, Miller & Remeika, 1962).

In reciprocal space, the normal phase shows difference reflexions with quarter-integral  $k$  indices, while

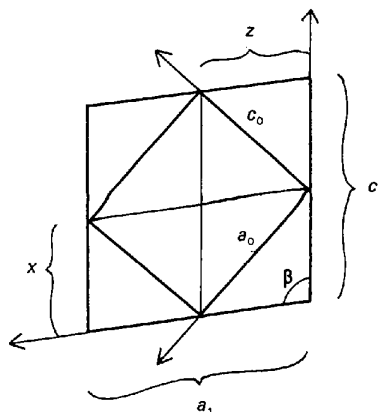


Fig. 1. Relation of pseudocubic axes as used in this paper (subscript 1) and conventional orthorhombic axes (subscript 0); senses are shown by the arrows. Both  $b_1$  and  $b_0$  are vertically upwards from the paper;  $b_0 = b_1 = 4y$ .

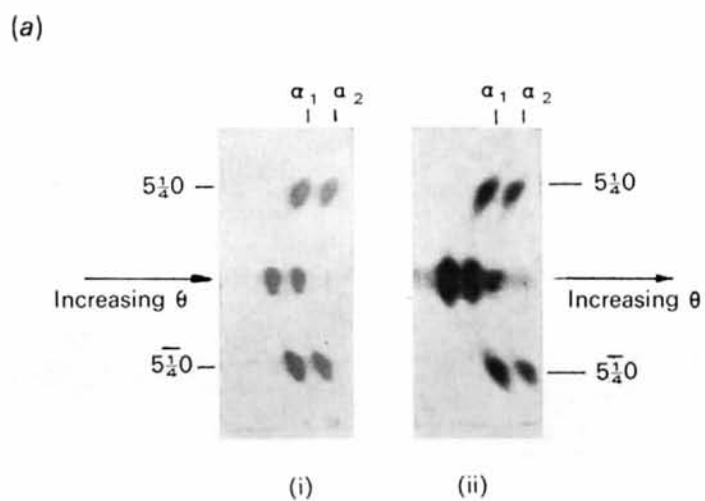


Fig.2. Enlargements of parts of oscillation photographs at high Bragg angle. (a) Coexistence of phases *P* and *Q*: (i) phase *P* alone, with *b* parallel to axis of rotation, showing 500,  $5\frac{1}{4}0$ , and  $5\frac{1}{4}0$ ; (ii) phases *P* and *Q*, the latter showing only 500, otherwise as (i).

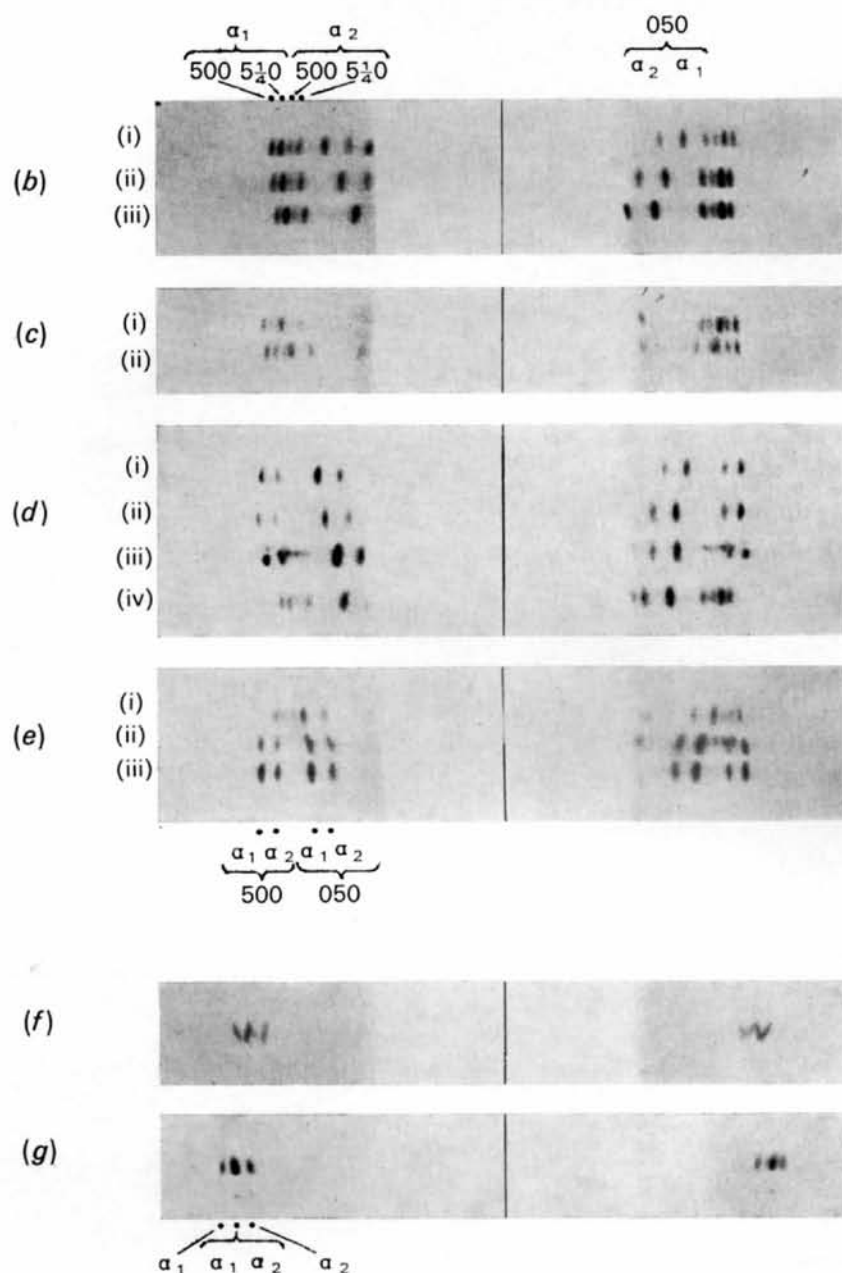


Fig. 2. (cont.) (b) Thermal expansion in phase *P*: (i) 145°C, (ii) 75°C, (iii) room temperature. Notice the 'interleaved doublet' of 500,  $5\frac{1}{2}0$ , and the displacement of 050 outward towards 500 with increasing temperature. (c) Thermal expansion in phase *P*: (i) 310°C, (ii) 280°C. Notice the overlap of the 050 and  $5\frac{1}{2}0$  doublets, and the greater slope of 050. (d) Transition *P* → *Q*: (i) 190°C, phase *Q*, (ii) 145°C, phase *Q*, (iii) 125°C, two-phase, (iv) 90°C, phase *P*. Notice the difference between (d) (ii) and (b) (i), which are at the same temperature in the same run, but at different azimuths, *i.e.* from different domains. (e) Transition *Q* → *P*: (i) 250°C, phase *P*, (ii) 220°C, two-phase, (iii) 220°C, photograph immediately preceding (ii), phase *Q*. (f) Phase *W*, about 505–525°C. Notice opposite slopes of two doublets. (g) Phase *T*, about 630°C. Notice larger slope of inner doublet, corresponding to larger expansion of smaller spacing. (The central hole for the admission of the collimator has been blotted out on the prints; in each of (b)–(e), separate original photographs were superposed with a vertical displacement, and the reproduction was made from the composite negative, the centre line being added on the print. In some of the photographs, the  $\alpha_1$  of  $5\frac{1}{2}0$  has lain within the oscillation range, and can be seen lying nearer the centre than the  $\alpha_2$  of 050.)

phase II has half-integral. These are useful identifying features. The appearance and relative positions of 500,  $5\frac{1}{2}0$ , (or 005,  $0\frac{1}{2}5$ ), which have Bragg  $\theta$ 's of about  $80^\circ$ , are particularly useful criteria [Fig. 2(a)–(e)].

### 1.6. *Twinning and twin textures*

In the perovskite family, one may reasonably look for twin components in any orientation which interchanges any of the subcell edges  $x$ ,  $y$ ,  $z$ , with or without reversal of direction. This kind of mimetic twinning brings together in reciprocal space, and hence on the photograph, reflexions which belong to the same form in the aristotype. We refer to such a group as a *spot complex*, and give it the indices of the corresponding aristotype reflexion. Only at high  $\theta$  values are the individual reflexions sufficiently well resolved to be interpreted. A complicated group may offer some initial difficulty, but once its separate spots are correctly indexed (with information derived from simpler photographs) it can help very much in two ways: (i) in improving accuracy, since small separations or 'splittings' on the photographs can give spacing differences in which certain systematic errors are eliminated; (ii) in counteracting the effect of preferred orientation, which might otherwise mean that one of three different spacings could be overlooked.

In the room-temperature form, the simplest type of twinning, studied by Wood (1951), is about the normal to (100). In reciprocal space, 500 and 050 remain single, but 005 has two components with equal spacing but about  $1\frac{1}{2}^\circ$  angular separation in the  $[h0l]$  zone; 403 and  $40\bar{3}$ , with different spacings, are juxtaposed. Multiple twinning about the same axes produces parallel lamellae in the crystal, as described by Wood, with no further complexity in reciprocal space. By symmetry, however, similar effects can occur with the (001) normal as twin axis. If only one axis is used, we call it 'simple type-1' twinning; if both are used, 'double type-1' twinning.

Twinning is also possible about the normal to (110) or symmetry-equivalent directions. In the  $[hk0]$  zone, this brings together 500 and 050, 430 and 340. This kind of twinning is called 'type-2'.

We are not concerned here with a detailed study of the twin laws, except so far as they give rise to particular arrangements in spot complexes, and help to elucidate the symmetry. Type-1 twinning is only possible when the axes are non-orthogonal; its most characteristic effect is the  $403/40\bar{3}$  splitting. Type 2 can occur whenever any direction of the form  $\langle 110 \rangle$  in the aristotype is not a symmetry direction.

## 2. Experimental

### 2.1. *Outline of method, and samples studied*

Each crystal studied was enclosed in a silica-glass capillary and heated in a miniature furnace consisting of a few turns of platinum wire mounted on the goniometer arcs (Lefkowitz & Megaw, 1963).

It was essential, in order to avoid misinterpretations, to test the reproducibility of results as widely as possible. A number of different crystals were examined, most of them in repeated temperature runs. Weissenberg, oscillation, and back-reflexion photographs were taken, some with Cu  $K\alpha$  and some with Mo  $K\alpha$ . In one run, optical observations with crossed polaroids were also made.

The most detailed work was done with crystal 1, about 2 mm high and 0.5 mm square in cross-section, comprising several large domains with fine striations of lamellar twinning. For this, Cu  $K\alpha$  radiation and the van Arkel film mounting were used. Crystal 2, rather larger and more extensively twinned, gave additional information above  $500^\circ\text{C}$ . Crystal 3, of about 0.3 mm side, originally showed only type-1 twinning, but gave also type-2 twinning after heating to  $700^\circ\text{C}$ . Two small good crystals of less than 0.1 mm side were also used; one had a very small type-2 twin component, and the other was originally single but developed simple type-1 twinning on being inserted in the furnace.

### 2.2. *Temperature control and calibration*

An arbitrary temperature scale for any run was given by the setting of the variac controlling the furnace current. Conversion to a true scale was not easy, because with such a small furnace the thermal equilibrium was affected by conduction either along the specimen itself (and its mount) or along any probe put in to examine it. A calibration with aluminum powder mounted beside crystal 1 located the two main transitions at  $360^\circ\text{C}$  and  $600^\circ\text{C}$ , with a linear scale between them; the calculated temperature had a precision of  $\pm 3^\circ\text{C}$ , but the sensitivity of the variac setting was not better than  $\pm 10^\circ\text{C}$  in the upper temperature range. The 'aluminum scale' was accepted as correct up to  $360^\circ\text{C}$ , and modified in the upper range by taking the upper transition temperature as  $640^\circ\text{C}$  and using linear interpolation. Other crystals were calibrated by comparison with crystal 1. An internal check was provided by the rather sharp  $520^\circ\text{C}$  transition (see § 5.1), which was not used as a fixed point, yet in each run occurred at very nearly the same temperature.

### 2.3. *Temperature variations*

Variations of temperature with time during the taking of a photograph, which would have broadened the reflexions, were never great enough to be noticed. On the other hand, variations within the part of the crystal illuminated were very important. On oscillation photographs their magnitude could be estimated from the slopes of the reflexions, which were found to be correlated with the thermal expansions (See Fig. 2(c); the effect is more noticeable on the right hand side). The top of the crystal was always hotter than the bottom; the difference increased with temperature; it was consistent (though not identical) for both azimuths; and it was reproducible in all runs with the same crystal.

On Weissenberg photographs similar effects were recognisable.

These effects set a limit to the precision of temperature measurement – less serious in the lower temperature range but rising to perhaps  $\pm 20^\circ\text{C}$  at the upper end – but by allowing direct observation of the thermal expansion they provided in practice a most powerful tool for elucidating the system.

#### 2.4. Spacing measurements and accuracy

All accurate measurements were made with the 500 or 430 spot complex, both of which occur at a Bragg angle of about  $80^\circ$ . Good spots on photographs with van Arkel mounting could be measured to give an accuracy of  $\pm 0.0001 \text{ \AA}$ . With complex or ill-shaped spots, or simple hand measurement of Weissenberg photographs,  $\pm 0.0010 \text{ \AA}$  was still attainable.

Systematic errors might be due to (i) errors in effective camera radius (including those due to eccentricity of the specimen, absorption, and film shrinkage), (ii) effects of angular mis-setting. Detailed consideration shows that errors due to (i) are not likely to be greater than  $\pm 0.0010 \text{ \AA}$ . Angular mis-setting is more serious, particularly as it can occur at a transition in the middle of a run. Large mis-settings can be seen by inspection, and the measurements rejected, but errors up to about  $0.0025 \text{ \AA}$  in the higher part of the range of spacings might pass unrecognized.

All systematic errors were very much reduced when spacing differences were calculated from the same spot complex on the same photograph, and this was done whenever possible. The disadvantage is that resolution was limited by the individual spot width, and was rarely better than  $0.007 \text{ \AA}$ .

Altogether, limits of error\* for the upper temperature range might be set at  $\pm 0.0020 \text{ \AA}$ ; below about  $280^\circ\text{C}$ , where the angular mis-setting danger was less, and the spots better shaped, they drop to  $\pm 0.0007 \text{ \AA}$ .

#### 2.5. Interaxial angles

For the room-temperature phase,  $\beta$  can accurately and conveniently be calculated from the differences of Bragg  $\theta$  for 403 and  $40\bar{3}$ , recorded on Weissenberg photographs. We have

$$\sin\left(\beta - \frac{\pi}{2}\right) = \frac{25}{24} \frac{\sin^2\theta(403) - \sin^2\theta(40\bar{3})}{\sin^2\theta(403) + \sin^2\theta(40\bar{3})}$$

Since  $\beta - \pi/2$  is less than  $1^\circ$ , and the  $\theta$ 's are about  $80^\circ$ , we may approximate and simplify. Writing the Bragg angles as  $\theta \pm \frac{1}{2}\Delta\theta$ , we obtain

$$\beta - \frac{\pi}{2} = \frac{25}{24} \Delta\theta \left(\frac{\pi}{2} - \theta\right) \left\{1 + \frac{1}{3} \left(\frac{\pi}{2} - \theta\right)^2\right\}.$$

The accuracy of  $\Delta\theta$ , which depends on the accuracy of the interspot distance, controls the accuracy of the result. Careful measurement with a travelling micro-

scope gave limits of  $\pm 0.2'$ , simple measurements with a ruler and hand lens limits of  $\pm 1'$ . (The error introduced by the approximation is less than  $0.1'$ .)

An alternative way of measuring  $\beta$  used the oscillation photographs originally taken to study the 500 complex of crystal 1, where pairs of reflexions such as  $112/1\bar{1}\bar{2}$  were brought together on the layer lines by twinning. This method was much less accurate than the other.

### 3. Results: outline

Spacings are plotted as a function of temperature in Figs. 3 and 4. (For orthogonal cells, spacings are of course equal to subcell edges; but since spacings are the directly observed quantities, and subcell edges are deduced from them by knowledge, or assumption, of interaxial angles, it seemed preferable to record results in terms of the former.) Though it was not practicable to plot measurements individually in Fig. 4, all values agreed with the smooth curves within the expected error limits†.

Interaxial angles are plotted in Fig. 5. Above  $360^\circ\text{C}$  there was no evidence of any departure from orthogonality, either from  $403/40\bar{3}$  separations or from spot-splitting on higher layer-lines of oscillation photographs; angles measured directly on Weissenberg photographs confirmed this less sensitively.

It is not immediately obvious from Fig. 4 just how many phases are found. However, different temperature ranges are clearly characterized by particular features of the set of subcell parameters, and these, listed in Table 1, column 3, serve for definition. The phase (or sequence of phases) corresponding to each such range is named with a serial letter (column 2). (Names used by previous workers have been deliberately avoided for fear of confusion.) If further, less obvious, breaks within any range are recognized later, the different phases can be distinguished by subscripts. A summary of the further information available is given in column 4; more detailed discussion follows in the remaining sections of the paper.

Thermal expansions in the different temperature ranges are summarized in Tables 2 and 3.

Very marked changes of texture occurred during some of the runs, particularly on cooling. Near  $520\text{--}500^\circ\text{C}$ , systematic changes of tilt of as much as  $20^\circ$  between domains were observed in one run; and abrupt appearance and disappearance of spots due to misaligned domains occurred at several different temperatures between  $520^\circ\text{C}$  and  $640^\circ\text{C}$ . Annealing effects, sometimes involving reduction of misalignment and sometimes the fusion of separate misaligned domains, were commonly observed. Such reorientation effects do not, by themselves, mark a transition. Almost certainly they are after-effects of a transition, but as their immediate cause may be the build-up of mechanical

\* The term 'limit of error' is not used to mean 'outside limit', but 'a 70% confidence limit, qualitatively comparable to a standard deviation'.

† See the report mentioned on p. 670 for tables of individual measurements and detailed comments.

Table 1. *High temperature phases of sodium niobate*

Approximate temperature range	Phase	Characteristics of subcell parameters*	Symmetry (if known) and further details
20–360°C	<i>P</i>	Two equal spacings of small thermal expansion at an angle slightly different from 90°; one smaller spacing, at right angles to the others, with multiplicity 4 and large thermal expansion.	Orthorhombic in rhombic orientation; detailed structure known (Lukaszewicz, Sakowski & Megaw).
(20–?)260)	<i>Q</i>	Like <i>P</i> , but large spacings larger by 0.007 Å, and smaller spacing with multiplicity 2.	Orthorhombic in rhombic orientation; detailed structure known (Wells & Megaw)
360–440	<i>R</i>	Orthogonal; one large spacing of small thermal expansion, and two nearly equal small spacings of large thermal expansion.	Orthorhombic in parallel orientation; upper limit uncertain.
440–518	<i>S</i>	All spacings nearly equal; two have difference of about 0.002 Å and large thermal expansion.	May be two phases, <i>S</i> <sub>1</sub> and <i>S</i> <sub>2</sub> , with a spacing anomaly between them at 480°C.
518–526	<i>W</i>	Very narrow temperature range; large spacing with large positive thermal expansion, and smaller spacing with large <i>negative</i> thermal expansion.	Perhaps only stable when clamped (see text).
526–640	<i>T</i>	Two spacings with difference of about 0.010 Å; overall thermal expansions of both large and nearly equal.	Probably at least 2 distinct phases; may be 3 or 4. Possibly tetragonal above 580°C, but not below.
Above 640°C		Cubic; all multiplicities unity.	The aristotype.

\* The subcells are described in terms of their interplanar spacings (perpendicular distances between subcell faces) rather than their subcell edges, because the former are more directly related to observation.

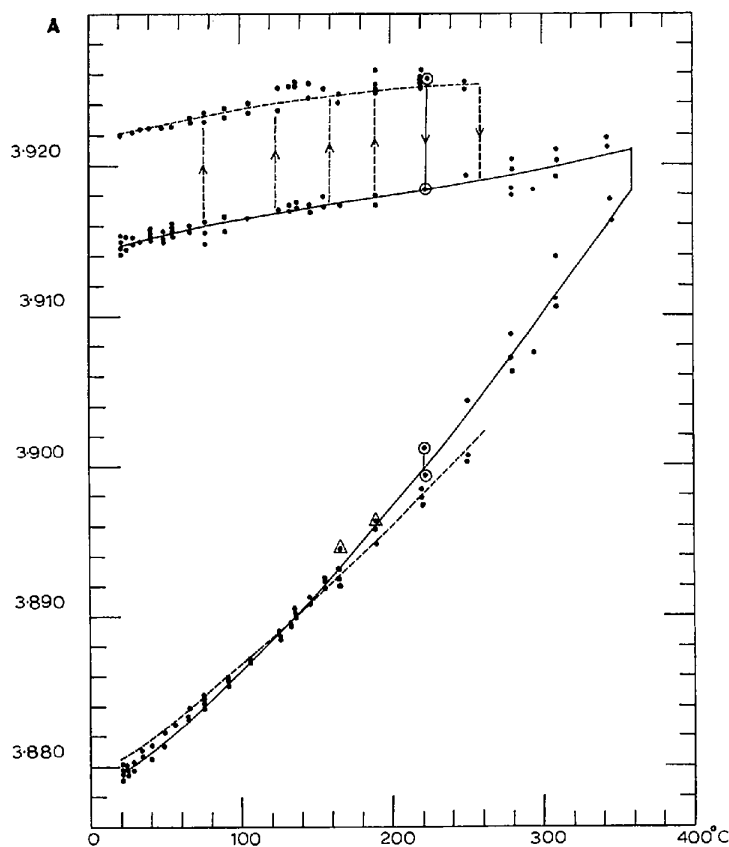


Fig. 3. Spacings  $x \sin \beta$  and  $y$  as a function of temperature, up to 360°C. Full line *P*, broken line *Q*. Points are measurements from individual spots or  $\alpha_1/\alpha_2$  doublets on photographs; circled points, measurements from one photograph (see text). Vertical lines indicate temperatures where transitions occurred.



Table 2. *Thermal expansion coefficients in phase P* ( $\text{deg}^{-1} \times 10^{-6}$ )

	$x \sin \beta$	$y$	$\beta$	[10 $\bar{1}$ ] direction (orthorhombic $a_0$ )	[101] direction (orthorhombic $c_0$ )
Average over range	4.6	29.3	-14.8	-2.8	+12.0
At 20°C	4.6	22.6	-6.9	+1.1	+8.1
At 360°C	4.6	34.7	-19.4	-5.1	+14.1

Table 3. *Thermal expansions*

Temperature range	Phase	$\alpha_x$	$\alpha_y$	$\alpha_z$	Comment
		$(\text{deg}^{-1} \times 10^{-6})$			
20-360°C	<i>P</i>	5	29	5	See text.
340-440	<i>R</i>	23	26	3	
440-470	<i>S</i> <sub>1</sub>	?	26	34	Identification of spacing rather doubtful.
470-518	<i>S</i> <sub>2</sub>	?	?	41	
518-526	<i>W</i>	-70	80	64	Order-of-magnitude only; possibly includes effect of discontinuities (see text).
530-580 } 580-600 } 600-630 } 630-640 }	<i>T</i>	{ 36 27 31 62	{ 6 ? ? ?	{ 24 25 0 -70	Over-all values.  Temperature interval uncertain; possibly includes effect of discontinuities.
640-800	Cubic	12.7			
340-640		23			Over-all average for intermediate spacing.

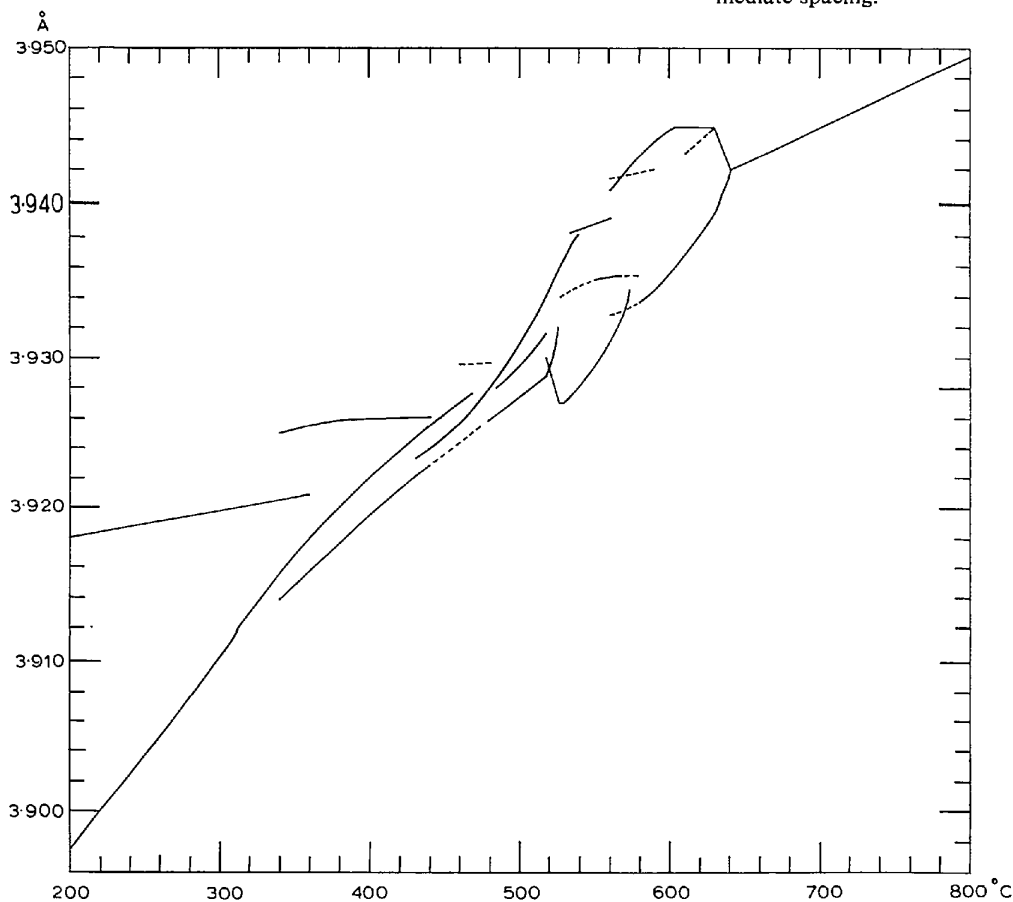


Fig. 4. Spacings as a function of temperature, from 200°C to 800°C. (Note that where thermal hysteresis occurs there may be two phases coexisting over a temperature range, and therefore more than three observed spacings.)

(and perhaps electrical) stresses with thermal expansion over an undefined temperature interval, their evidence must be used with considerable caution.

#### 4. Temperature range 20°C – 360°C

##### 4.1. Existence of two phases

All measurements lay on the smooth curves of Fig. 3, within the expected limits of error, except for minor anomalies near 140°C and 240°C discussed below.

Two different phases *P* and *Q* occur. Phase *P* is the normal room-temperature phase, and phase *Q* has essentially the same diffraction pattern as phase II of Wells & Megaw (1961) and is almost certainly identical with the 'forced ferroelectric'. The two are readily distinguishable by the occurrence of  $5\frac{1}{2}0$  reflexions with *P*, and their absence with *Q* [Fig. 2(a), (d), (e)].

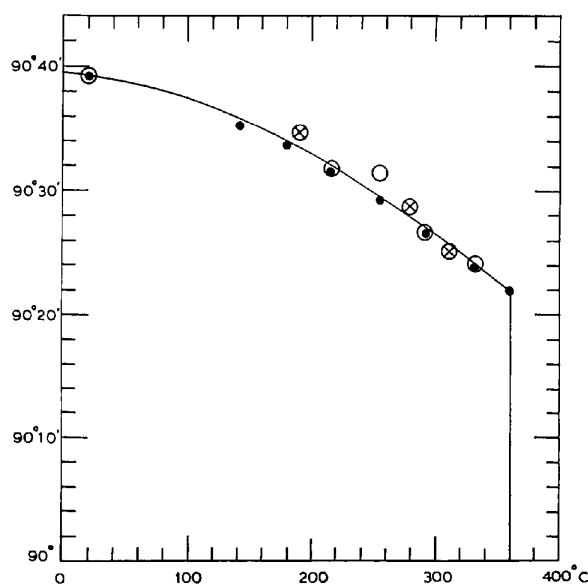


Fig. 5. Interaxial angle  $\beta$  for phase *P*. Differently marked points are from different runs: dots are measurements to within  $\pm 0.2'$ , circles to within  $\pm 1'$ .

The only obvious difference in the spacings of the two phases is in  $x \sin \beta$ , which is greater for *Q* by about  $0.007 \text{ \AA}$ . There is probably a very small difference in the  $y$ 's near 240°C (see § 4.3), but at room temperature they are indistinguishable.

##### 4.2. Thermal expansion of phase *P*

There is a striking difference between the thermal expansions of  $x \sin \beta$  and  $y$  (Table 2). Its effect can be seen in Fig. 2(c) in the different slopes of the 500 and 050 spots, as well as in the relative movement of the two spots between photographs at different temperatures.

The interaxial angle  $\beta$  has a steady decrease with increasing temperature, followed by a discontinuous fall to 90° at 360°C (Fig. 5).

The principal expansion coefficients in the (010) plane are given (within an accuracy of 1%) by

$$\frac{1}{x \sin \beta} \frac{d}{dT} (x \sin \beta) \pm \frac{1}{2} \frac{d\beta}{dT}$$

where the + and – signs refer to  $[10\bar{1}]$  and  $[101]$  respectively (the long and short diagonals of the rhomb). They are evaluated in Table 2. The negative coefficient for  $[10\bar{1}]$  is rather striking. Nevertheless it is possible that description in terms of the principal coefficients has less physical meaning than the simpler description in terms of  $\beta$  and  $x \sin \beta$  separately, the coefficient derived from  $x \sin \beta$  being (within 1% accuracy) the mean linear expansion coefficient in the (010) plane.

##### 4.3. Occurrence and features of phase *Q*

The occurrence of phase *Q* is not reproducible, nor are the conditions of its formation known. It cannot yet be prepared at will. A summary of its occurrences in crystal 1 is given in Table 4; it was found at room temperature in a number of other large crystals from two different sources [sometimes coexisting with *P* – see Fig. 2(d)(iii), (e) (ii)] but never in the small crystals studied in the later stages of the work. One possibility is that it needs the inter-domain clamping stresses ex-

Table 4. Occurrence of phases *P* and *Q* in sodium niobate (crystal 1)

Run*	Transition temperature		Comment
	<i>P</i> → <i>Q</i>	<i>Q</i> → <i>P</i>	
14A	75°C	Not examined	Small spots due to <i>Q</i> visible from room temperature upward. More equally two-phased at 75°C; thereafter only <i>Q</i> . Remained <i>Q</i> immediately after cooling, but had reverted to <i>P</i> next day.
15B	—	220°C	<i>Q</i> at room temperature. The third successive photograph at 220°C [Fig. 2(e)(ii)] was two-phase showing <i>P</i> and <i>Q</i> .
17A	160°C	260°C	} Different <i>P</i> → <i>Q</i> transition temperatures for two components of 'twin'; <i>Q</i> → <i>P</i> between 250 and 280°C for both.
17B	125°C	260°C	
18A	190°C	Not examined	Faint appearance at 190°C; at 210°C only <i>Q</i> .

\* The letter *A* or *B* after the run number refers to the azimuth at which the crystal was examined during that run. In run 17, the two azimuths were examined successively.

isting in a large crystal to stabilize it in the absence of a field.

In Fig. 3, there seems to be a small break in the  $y$  curve near  $260^\circ\text{C}$ . The anomalous points below this temperature all belong to phase  $Q$ . The pair of points encircled at  $220^\circ\text{C}$ , and the corresponding pair for  $x \sin \beta$ , all came from one two-phase photograph [Fig. 2(e) (ii)], in which the 050 differences, though less than the 500 differences, were visible to the eye. (The sharpness of detail has been lost in the reproduction.) These facts suggest a real, though small, difference between  $y_Q$  and  $y_P$ .

In view of the experimental scatter which begins to be important above  $280^\circ\text{C}$ , a confirmatory test was needed. On the hypothesis that  $y_P = y_Q$ , the ratio  $(x \sin \beta)/y$  was calculated from Fig. 3 for both phases, using the full and broken lines for  $x \sin \beta$  and the full line only for  $y$ . The results were plotted as the full lines in Fig. 6. In Fig. 6 are also plotted, as points or crosses, all axial ratios calculated from juxtaposed spots in the same photograph; for these, errors of crystal setting are eliminated or greatly reduced. For  $P$ , all points now lie close to the full line – note in particular the great reduction in scatter above  $280^\circ\text{C}$  – but for  $Q$  above about  $180^\circ\text{C}$  they are systematically above it in all runs. Hence  $y_Q$  is less than  $y_P$  from about  $180^\circ\text{C}$  to  $260^\circ\text{C}$ .

The broken curve in Fig. 6 has been drawn empirically through the points, and the broken curve for  $y_Q$

in Fig. 3 has been calculated from it. Differences between the  $y_P$  and  $y_Q$  curves below about  $180^\circ\text{C}$  are not significant.

The small anomaly seen in Fig. 3 for  $x \sin \beta$  near  $140^\circ\text{C}$  was observed in one run for temperatures where the crystal was in a two-phase state. It probably represents a small experimental error due to changes in relative tilt of domains.

The interaxial angle  $\beta$  is known with less accuracy than for  $P$ , as it was measured only from layer-line spot separation (§ 2.5). The value for  $Q$  is approximately equal to that for  $P$ ; it may be about  $6'$  less at room temperature, but this estimated difference is very doubtfully significant.

#### 4.4. Nature of $P \rightleftharpoons Q$ transition

It is clear that the  $P \rightleftharpoons Q$  transition is not a simple equilibrium one – the thermal hysteresis is much too large. On the other hand, an explanation of the observed effects as due to slight differences of experimental arrangement by which the X-ray beam is displaced relative to a permanent boundary separating the two phases is certainly not adequate; at the very least, there is a temperature-dependent movement of the domain boundary. The effect could be described in more general terms by saying that the free-energy curve of  $Q$  lies normally very little above that of  $P$  and nearly parallel to it, and changes in conditions – for example, the mutual clamping stresses of domains, or anisotropic

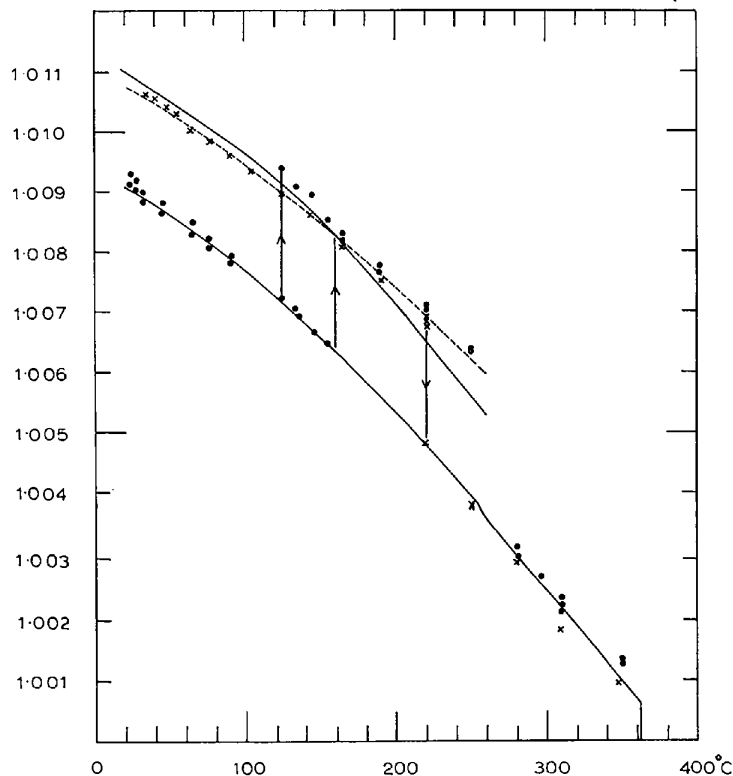


Fig. 6. Axial ratios of phase  $P$  (lower curve) and phase  $Q$  (upper curves). Full lines calculated from Fig. 3; broken line for  $Q$  fitted through points. Dots and crosses represent individual measurements from runs 17 and 15 respectively (cf. Table 4).

temperature gradients – can move them up and down relative to one another, making them intersect twice at temperatures which are very sensitive to their relative levels. The curves lie close together between room temperature and 280°, but separate more widely above (Fig. 7). This, however, is only an alternative description in phenomenological terms, and does not help us to understand the origin of the effect, which remains obscure.

#### 4.5. Comparison with other work

Our lattice parameter measurements for phase *P* are in substantial agreement with those of SNP (1954) and SVŽ (1961). The axial ratios of SVŽ are rather lower than ours, probably because the imperfect resolution of their overlapping peaks was not fully allowed for.

Possible occurrences of a ferroelectric phase in pure  $\text{NaNbO}_3$  at room temperature have been suspected previously (Shafer & Roy, 1959; see also WMR (1962) for other references). Pulvari (1960) reported the existence of hysteresis-loops between room-temperature and 225°C from a vanadium-containing material, which was subsequently shown by Miller, Wood, Remeika & Savage (1962) to be indistinguishable in its other dielectric behaviour from pure  $\text{NaNbO}_3$ ; there was an anomaly at 225°C, which might well be explained by a  $Q \rightarrow P$  transition. In none of this work was the identity of the *Q*-phase clearly demonstrated and no parameter measurements were made. Our specimen was not analysed chemically to test for possible traces of impurity.

The structure of  $\text{AgNbO}_3$  is isomorphous with that of  $\text{NaNbO}_3$  (Francombe & Lewis, 1958). Its lattice parameters are very similar, and there is a discontinuity in  $\beta$  at the 325°C transition. Weak ferroelectricity was reported, together with unexplained peaks in the dielectric constant curves not corresponding to any obvious change of structure. These facts may just possibly indicate the occurrence of  $P \rightleftharpoons Q$  transitions as in  $\text{NaNbO}_3$ .

## 5. Temperature range 360°C – 640°C

### 5.1. Lattice parameters

Immediately above 360°C is phase *R*. There are three distinct spacings, and the interaxial angles are all 90°. The axial directions (here and also for all higher-temperature phases) are named to give the relation  $z > y > x$ . The low thermal expansion of  $z_R$ , and the

high expansions of  $x_R$  and  $y_R$ , are characteristic features, visible on Weissenberg photographs.

The transition  $P \rightleftharpoons R$  tended to occur in an oriented and reversible way in good crystals, with  $y_P \rightleftharpoons y_R$ . One crystal which was single in phase *R* and had simple type-1 twinning in phase *P* preserved these characters through a number of temperature cycles, though the ratios of the volumes of the twin components varied unsystematically; the normal to the twin plane had the direction of  $x_R$ .

At the upper end of phase *R*, all three spacings have become nearly equal, and it is difficult to be sure of the transition temperature, which is taken rather arbitrarily as 440°C.

The near-equality of the spacings persists to about 520°C, and this region is called *S*. There are certainly at least two different spacings with thermal expansions which are roughly equal and rather large, but their relation to the third spacing, and the nature of the small observed anomaly at 480°C, remain doubtful.

At about 520°C very marked changes of spacing occurred within a narrow temperature range of about 10°C, reproducibly with different crystals. The phase was called *W* because of the characteristic appearance of the complex spots on oscillation photographs [Fig. 2(f)]. The largest spacing,  $z_W$ , showed a rapid continuous increase with increasing temperature; another,  $x_W$ , showed a nearly equally rapid decrease. Possibly there are also small discontinuities at the temperature limits, masked by effects of spot width. The third spacing,  $y_W$ , was only observable in the heavily twinned crystal 2, suggesting a preferred direction parallel to the length of a good crystal.

From about 530°C to 600°C – the main part of the *T* range – the extreme spacings  $z_T$  and  $x_T$  had (over-all) high positive thermal expansions. An intermediate spacing  $y_T$  of low thermal expansion was clearly detectable in some runs, but nearly always in the weaker component of a twin; apparently its preferred orientation is parallel to the length. Above about 580°C only two spacings could be detected with certainty, but there was some evidence that the third was equal or nearly equal to the larger of the others. From 600°C–630°C the low thermal expansion of  $z_T$  was conspicuous on oscillation photographs [for example, on the original of Fig. 2(g)]. Whether the changes at 600°C and 630°C were gradual or associated with a discontinuity in spacing or in thermal expansion cannot be said with certainty.

### 5.2. Optical observations

Observations were difficult to make through the capillary, and unfortunately it proved impossible to be sure whether the same domains were being observed optically and by X-rays. The following points were noted: (i) A very striking change was seen at about 440°C: the multiple twinning of the room-temperature phase, whose domain pattern had continued up to this temperature (in spite of the switch of extinction direc-

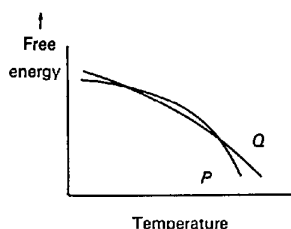


Fig. 7. Sketch diagram of free energy curves of *P* and *Q*.

tions at 360°C) suddenly disappeared here. (ii) Between 500°C and 540°C, the azimuth at which one large domain appeared nearly isotropic switched through 90°, the other azimuth showing straight extinction. (iii) On cooling to about 600°C, one domain appeared to show symmetrical extinction – the single exception to the rule that above 360°C straight extinction only was observed.

### 5.3. Difference reflexions

Difference reflexions were observed at all temperatures up to about 550°C, above which they were either absent or very weak. No systematic studies were completed, but, except in phase *R*, all reflexions above 360°C could be satisfactorily indexed with half-integral *h*, *k*, and *l*. Phase *R* showed, in addition to weak reflexions with half-integral indices, other very characteristic reflexions with indices *h*,  $k \pm \frac{1}{6}$ , *l*, only visible for *l* large. The  $0\frac{1}{2}5$  reflexions were particularly noticeable, as they replaced the  $5\frac{1}{4}0$  of phase *P*, though slightly weaker.

### 5.4. Comparison with other work on lattice parameters.

Our results are in excellent agreement with those of Francombe (1956), and (apart from a small unexplained systematic difference above 500°C) also in good agreement with those of SVŽ (1961) above 430°C, though we add new details. Small discontinuities near 430°C and 470°C were noted by SVŽ, as by us, though the character of their 430°C effect is different from ours.

Apparent discrepancies between the above results and the previous work of Wood (1951) and SNP (1954) can be explained by the fact that the resolution of the earlier workers was too low to detect spacing differences in the *S* range, and that they therefore did not try making measurements in the *T* range. Agreement with SNP in the *R* range is satisfactory.

There is disagreement with the work of Ismailzade (1963), who made counter diffractometer measurements of the powder-line profile of the 300/122 complex, at  $\theta \simeq 45^\circ$ . Probably the fault lies in his apparent assumption that the separate peaks of this complex at all temperatures can be indexed by analogy with the indexing at room temperature – which is certainly not legitimate. Correct indexing might give quite different lattice parameters. Nevertheless the discontinuities noted may be real, if they are based on direct observation and not on calculation; they occur at 420°C, 480°C, 515°C, and 570°C.

The other serious disagreement is with the work of SVŽ in the *R* range. From a splitting of the powder line 222 unaccompanied by more than a slight broadening of 400, these authors deduced a phase of orthorhombic symmetry in rhombic orientation, with  $\beta$  dropping from 90° 16' at 360°C to 90° at 430°C. Our results give orthorhombic symmetry in parallel orientation, which is incompatible with that. If their observation is correct and cannot be explained by some anomalous

preferred orientation in their specimen, their material must have been in a different phase from ours. Ismailzade also finds a departure from 90°, though a much smaller one, but his conclusions are doubtful, as explained above.

## 6. Discussion of the phases above 360°C

### 6.1. Symmetry

In the early studies, it was natural to make the simplest possible assumptions about the symmetry; now that the complexity of the system is realized, we have to be more critical and reject all arguments based on such assumptions. Moreover, a knowledge of the symmetry is neither necessary nor sufficient to identify a phase; there may well be a sequence of different phases with orthorhombic symmetry, and definite knowledge of the symmetry generally comes very much later than the recognition of the existence of a distinctive phase. The history of these studies has shown that negative evidence, such as the failure to detect small differences of spacing, is an unsound foundation for conclusions. The attempt to use 'orthorhombic', 'tetragonal', and 'pseudotetragonal', as definitive terms in this system has only caused confusion and should be abandoned, still more so the misleading term 'pseudo-monoclinic'.

All the optical evidence is in favour of orthogonal symmetry from 360°C to 640°C (with the exception of our one observation at 600°C). Our X-ray evidence, and that of SVŽ, is against any deviations from 90° interaxial angles, which were specially searched for; if any exist, they are small, and probably found only over limited temperature ranges. The most detailed optical work (CN 1955) shows a triaxial indicatrix over the whole temperature range from 360°C to 640°C, with parallel extinction, which implies orthorhombic symmetry in parallel orientation. SVŽ, in arguing for tetragonal symmetry in the 430°C–520°C range, give no reason for ruling out orthorhombic-parallel. Our X-ray work shows the existence of three different spacings in the 540°C–580°C range, and gives indications that at other temperatures the earlier reports of equal spacings were an over-simplification. Most of the reports of tetragonal symmetry were based on such negative evidence. At present it seems most likely that all phases from 360°C to 580°C, and perhaps to 640°C, are orthorhombic in parallel orientation; if the phase at 600°C is tetragonal, it probably has its smallest spacing in the direction of the unique axis, *i.e.*  $c/a \simeq 0.998$ . The possible existence of non-orthogonal phases cannot be completely ruled out, but there is no convincing evidence for any such.

### 6.2. Phase transitions

There is general agreement on the existence of the 360°C transition, detected by every investigating technique which has been tried.

The 430–440°C transition is rather doubtful. It has been noted in three modern X-ray studies (SVŽ, Ismailzade, and our own), but described differently in each; our optical observation is the only other evidence for it. We cannot regard its existence as proved.

The 470°C–480°C transition is again reported in the three X-ray studies and also in all the studies of optical birefringence. The temperature of the transition is subject to thermal hysteresis; the optical changes occur at lower temperatures on cooling. MR (1951) also noted a small peak in the dielectric constant near 480°C and so did CN (1954, 1955). There seems no doubt that a real, though small, change of phase occurs in this temperature region.

The 518°C and 526°C transitions are rather unusual. It seems certain from our photographs that, at least in large crystals, there is a narrow temperature range within which a negative thermal expansion of one spacing is found. The domains showing this were, however, certainly clamped between portions of the crystal at different temperatures and perhaps in different phases. It is possible that what we have called phase *W* can only exist in such circumstances – that it is only stable when there is either a temperature gradient or a particular type of mechanical stress due to clamping by other domains.

This is not really a surprising idea, because transitions involving very small geometrical changes are obviously likely to be sensitive to other thermodynamic variables than temperature and hydrostatic pressure. If it is the true explanation, then what we have called a thermal expansion may in reality be a thermomechanical strain effect. Then the phase would be a sort of buffer phase, to smooth out the rather abrupt changes in individual lattice parameters between *S* and *T*. In a small crystal with few domains, the phase would not be stable, and the two transitions would coalesce into one; but if the strains introduced by *S*–*T* differences were too great, very considerable fragmentation into smaller domains might occur.

Detailed studies in the 520°C region were not made by the other X-ray workers, though both Francombe (1956) and SVŽ (1961) noted the onset of line splitting, characteristic of the *T* range, occurring near this. CN (1954, 1955) noticed a small peak in the dielectric constant near 520°C, and their optical work showed a transition at 518°C, whose features (studied in careful detail) are of particular interest. (It is puzzling that Wood (1951) and SNP (1954) failed to notice this transition optically, unless it was because of preferred orientation in their crystals.) Writing the principal refractive indices\* as  $\gamma > \beta > \alpha$ , CN found that below 518°C  $\gamma \simeq \beta$  and above 518°C  $\beta \simeq \alpha$ ; moreover, while  $\gamma$  kept the same orientation in both phases,  $\alpha$  and  $\beta$  were interchanged. In consequence, the section of low bi-

refringence (apparent isotropy) switched direction – as we also observed (§ 5.2.) Though unfortunately we could not determine experimentally the relations between  $x, y, z$ , on the one hand, and  $\alpha, \beta, \gamma$ , on the other, the qualitative similarity between the crossing-over of the spacings in Fig. 4 and the crossing-over of refractive indices found by CN is suggestive. It is not legitimate to *assume* that a small refractive index is associated with a large spacing (as it would be for a material undergoing homogeneous strain); it would be of great interest if the actual facts could be found in the present case.

Above 530°C, our results suggest the possibility of transitions at about 550°C and 575°C, and perhaps also at 600°C and 630°C. Of these, the 575°C break is supported by the strongest evidence; the change involved seems to be a sudden increase of  $y$  from near-equality with  $x$  at about 3.935 Å to near-equality with  $z$  at about 3.942 Å. Explanation of the effects at the other temperatures as due to time-dependent annealing of domain texture cannot be altogether ruled out (*cf.* § 3).

The only earlier spacing measurements suggesting a transition near 570°C are those of Ismailzade (1963), which (as explained in § 5.4.) must be treated with reserve. Francombe (1956) noted a sharp decrease in the intensity of difference reflexions above 560°C.

Very interesting results were obtained by differential thermal analysis by Reisman, Holtzberg & Banks (1958). At first they could only detect a peak at 354°C, then after several cycles one appeared at 630°C, and finally one at 562°C. The latent heats associated with them were 150, 75, and 50 cal.mole<sup>-1</sup> respectively, and no others could be found. The 562°C peak was, in the early cycles, spread over about 100°C, and cycling up to 1150°C at 1 deg.min<sup>-1</sup> was needed to sharpen it. They suggest that ‘the middle transition is subject to strain and only by repeated annealing could consistent results be obtained . . . The unusual X-ray behaviour between 480°C and 560°C would appear to result from strain’. Our interpretation is different. It seems likely that thermal methods detect not only the sharp release of latent heat at a transition, but also the slow release of domain-wall energy over a continuous temperature range. In poorly annealed samples much of the latent heat may be converted into domain-wall energy; this process is obviously linked with the existence of thermal hysteresis, which is effectively a form of supercooling and superheating. Thus, strain undoubtedly occurs and may mask or smear out transitions, but it cannot *cause* the lattice parameter effects, which must have an origin (yet to be discovered) in the details of the crystal structure.

All the latent heats are very small, and probably close to the lower limit of detection. (Shafer & Roy (1959) only observed those at 360°C and 640°C). Probably the failure to observe the other transitions by differential thermal analysis simply means that their latent heats are smaller still.

\* There is some ambiguity in CN's notation: they imply but do not state that they define  $\gamma > \beta > \alpha$  (as is conventional) and then name the directions of  $\gamma, \beta$ , and  $\alpha$  as *a, b*, and *c* respectively.

At first sight it is surprising that a transition so hard to detect by X-rays is the only intermediate transition observable by differential thermal analysis. Possibly the reason lies in the relative values of the spacing changes. At 562°C (with which we associate our 575°C transition) the volume change depends on the change in  $y$ , which is easily missed in the X-ray work because of the near equality of  $y$  with  $x$  and  $z$  respectively on either side of the transition; at 520°C, where there are large changes in individual spacings, their opposite signs mean that the volume changes are less.

The effects just below 640°C noticed in our work resemble those in the 520°C region, though the evidence is rather less clear. If phase  $W$  is a stress-sensitive buffer phase, another of the same kind may exist just below 640°C. It is perhaps significant that (as Cross notes) neither the 518°C nor the 640°C transition is affected by thermal hysteresis.

One may sum up by saying that (i) modern X-ray techniques are very sensitive indicators of small changes in lattice parameters, but cannot easily assign exact temperatures, (ii) optical studies are also good indicators, but depend on the provision of good crystals, (iii) dielectric-constant methods are unreliable at high temperatures, (iv) thermal methods are relatively insensitive, but give valuable complementary information, (v) methods using single crystals or lightly-twinned crystals are potentially the most informative, but may be misleading because of preferred orientation. Where thermal hysteresis occurs, the only fully reliable method would be one in which all orientations of a single domain were observed simultaneously; while that ideal is unattainable, one has to combine information from all available methods, recognizing their advantages and their limitations. The  $P/Q$  relations recorded in Table 4, where differently oriented domains had different transition temperatures, serve as a warning in this respect, and also as a reminder that elsewhere in the system there may be genuinely different phases rendered stable at the same temperature by different heating or cooling techniques, or conditions other than temperature. We have to avoid on the one hand over-facile assumption of such phases to explain apparent discrepancies, and on the other hand too ready elaboration of hypotheses based on the belief that they cannot occur.

### 6.3. Multiplicity of the unit cell

Except in phase  $P$ , where the multiplicity  $m_2=4$  has been known since the early work of Wood (1951), and in phase  $R$ , where we find  $m_2=6$ , there is no evidence in any of our work for multiplicities higher than 2. There do not seem to be any observations in the literature which would require higher values; the qualitative similarity between difference lines at room temperature and above 360°C does not need this assumption to explain it. The powder lines actually reported have quarter-integral values of  $N(=h^2+k^2+l^2)$ , implying half-integral indices. (For a discussion of some mis-

understandings on this point, see WMR (1962), p. 1278.)

We have found difference reflexions up to 540°C; Francombe noted them above 560°C, and SVŽ detected them at 600°C, though with greatly weakened intensity. The latter authors reported that the lines with  $N=2\frac{1}{2}$  and  $2\frac{3}{4}$ , *i.e.* the  $\frac{3}{2}10$  and  $\frac{3}{2}1\frac{1}{2}$  complexes, persisted with little relative change of intensity over most of the temperature range. This implies that all three multiplicities are 2, and that the lattice of every phase is either primitive or one-face-centred. The indices of reflexions noticed by us support the same conclusion.

### 6.4. Structural changes

The most obvious question to be asked is: at what temperature does the off-centre displacement of the niobium atom in its octahedron disappear? Because this is likely to be accompanied by large changes in the dielectric constant, various writers (*e.g.* Francombe & Lewis, 1957; SVŽ, 1961) have thought that it happens at the 360°C transition; on the other hand, CN (1955), discussing their experimental observations, thought the dipole moments had not disappeared at 360°C, and Cross (1956) from thermodynamic arguments based on rather doubtful analogies, suggested it happened at 520°C.

Our work does not give a final answer, but we think the details of the  $P \rightleftharpoons R$  transition indicate a reorientation of the dipoles rather than their disappearance, and further work is in progress to investigate this.

If it is assumed that the  $0\frac{1}{2}5$  reflexions of phase  $R$ , like the  $5\frac{1}{4}0$  reflexions of phase  $P$  which they replace, are mainly due to the Nb atoms, an estimate of the displacement can be made. Calculations like those of Megaw & Wells (1958) suggest that the Nb displacement along the (010) face diagonal has decreased from 0.17 Å at room temperature to about 0.11 Å at 360°C in phase  $P$ . In phase  $R$ , the displacement is still in the (010) plane, but in the [001] direction. Two simple models can account for the preliminary results, with Nb displacements as shown in Fig. 8. In both, the largest displacement is roughly estimated as 0.08 Å.

As yet, we can not tell the temperature at which the displacements eventually disappear. Whether this necessarily involves conspicuous discontinuities in spac-

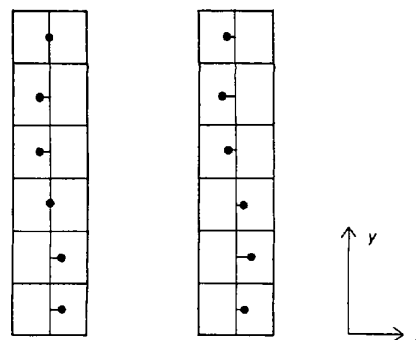


Fig. 8. Two possible models for the arrangement of Nb displacements in the unit cell of phase  $R$ .

ings, as is sometimes assumed, is by no means certain. Other transitions are undoubtedly due to puckering effects of the framework, but too little is yet known to make suggestions about their character. The possible role of the sodium atom in controlling their sequence has yet to be considered. Comparison with effects in  $\text{AgNbO}_3$  and  $\text{AgTaO}_3$  (Francombe & Lewis, 1958), which are obviously closely related, may be of considerable interest.

The results of this paper are therefore rather a clearing of the ground for future structural work than an answer to any detailed questions about the actual structures.

We wish to acknowledge the help of Miss P. Willard and Mrs T. Michalik in the measurement of photographs and computation of spacings. We are grateful to Mr P. Bradfield for taking one series of photographs and allowing us to use them. One of us (I. L.) is indebted for financial support to the U.S. Department of the Army, through its European Research Office, and one (K.Ł.) to the Polish Academy of Sciences for a Scholarship and leave of absence which made the visit to Cambridge possible.

#### References

- CROSS, L. E. (1956). *Phil. Mag.* (8), **1**, 76.  
 CROSS, L. E. & NICHOLSON, B. J. (1954). *Research Correspondence*, **7**, s 36.  
 CROSS, L. E. & NICHOLSON, B. J. (1955). *Phil. Mag.* (7), **46**, 453.  
 FRANCOMBE, M. H. (1956). *Acta Cryst.* **9**, 256.  
 FRANCOMBE, M. H. & LEWIS, B. (1957). *J. Electronics*, **2**, 387.  
 FRANCOMBE, M. H. & LEWIS, B. (1958). *Acta Cryst.* **11**, 175.  
 ISMAILZADE, I. G. (1963). *Kristallografija*, **8**, 363 (translated in *Soviet Phys. Crystallogr.*).  
 JONA, F. & SHIRANE, G. (1962). *Ferroelectric Crystals*. New York: Pergamon Press.  
 JONA, F., SHIRANE, G. & PEPINSKY, R. (1955). *Phys. Rev.* **97**, 1584.  
 LEFKOVITZ, I. & MEGAW, H. D. (1963). *Acta Cryst.* **16**, 753.  
 ŁUKASZEWICZ, K., SAKOWSKI, A. & MEGAW, H. D. In preparation.  
 MATTHIAS, B. T. (1949). *Phys. Rev.* **75**, 1771.  
 MATTHIAS, B. T. & REMEIK, J. P. (1951). *Phys. Rev.* **82**, 727.  
 MEGAW, H. D. & WELLS, M. (1958). *Acta Cryst.* **11**, 858.  
 MILLER, R. C., WOOD, E. A., REMEIK, J. P. & SAVAGE, A. (1962). *J. Appl. Phys.* **33**, 1623.  
 PULVARI, C. F. (1960). *Phys. Rev.* **120**, 1670.  
 REISMAN, A., HOLTZBERG, F. & BANKS, E. (1958). *J. Amer. Chem. Soc.* **80**, 37.  
 SHAFER, M. W. & ROY, R. (1959). *J. Amer. Ceram. Soc.* **42**, 482.  
 SHIRANE, G., NEWNHAM, R. E. & PEPINSKY, R. (1954). *Phys. Rev.* **96**, 581.  
 SOLOV'EV, S. P., VENEVCEV, YU. N. & ŽDANOV, G. S. (1961). *Kristallografija*, **6**, 218.  
 TENNERY (1965). *J. Amer. Ceram. Soc.* **48**, 537.  
 VOUSDEN, P. (1951). *Acta Cryst.* **4**, 545.  
 WELLS, M. & MEGAW, H. D. (1961). *Proc. Phys. Soc. London*, **78**, 1258.  
 WOOD, E. A. (1951). *Acta Cryst.* **4**, 353.  
 WOOD, E. A., MILLER, R. C. & REMEIK, J. P. (1962). *Acta Cryst.* **15**, 1273.

*Acta Cryst.* (1966). **20**, 683

## The Crystal Structure of Spermidine Trihydrochloride

BY E. GIGLIO, A. M. LIQUORI AND R. PULITI

*Istituto Chimico, Università di Napoli, and Centro Nazionale di Chimica delle Macromolecole (CNR) Sez. III, Napoli, Italy*

AND A. RIPAMONTI

*Istituto di Chimica, Università di Trieste, Trieste, Italy*

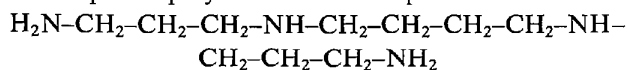
(Received 3 August 1965)

Crystals of spermidine trihydrochloride are monoclinic, space group  $Cm$ , with  $a = 27.58 \pm 0.02$ ,  $b = 5.42 \pm 0.01$ ,  $c = 4.62 \pm 0.01$  Å;  $\beta = 90^\circ 00' \pm 12'$ .

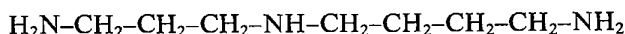
The crystal structure has been solved by analysis of the two-dimensional Patterson functions and then refined by several cycles of three-dimensional Fourier differential synthesis. The carbon and nitrogen atoms of the spermidine molecule lie in the mirror plane at  $y=0$  and the conformation of the chain is extended *trans* planar. Most of the hydrogen atoms have been located by means of a three-dimensional difference synthesis. The molecular packing is mainly determined by the closest contacts between nitrogen and chlorine atoms, which form hydrogen bonds.

#### Introduction

The aliphatic polyamines such as spermine



and spermidine



occur in several biological systems. Many studies have been made on the physiological and pharmacological